
Articles


1993

Hysteresis and Anchoring Energy in Ferroelectric Liquid Crystals

Yuri Panarin

Technological University Dublin, yuri.panarin@tudublin.ie

Follow this and additional works at: <https://arrow.tudublin.ie/creaart>

 Part of the [Condensed Matter Physics Commons](#), [Engineering Commons](#), [Engineering Physics Commons](#), [Fluid Dynamics Commons](#), [Optics Commons](#), and the [Other Physics Commons](#)

Recommended Citation

Panarin, Y. (1993). Hysteresis and Anchoring Energy in Ferroelectric Liquid Crystals. Gordon and Breach. DOI: 10.21427/1T6S-FZ03

This Article is brought to you for free and open access by ARROW@TU Dublin. It has been accepted for inclusion in Articles by an authorized administrator of ARROW@TU Dublin. For more information, please contact arrow.admin@tudublin.ie, aisling.coyne@tudublin.ie, gerard.connolly@tudublin.ie, vera.kilshaw@tudublin.ie.



This work is licensed under a [Creative Commons Attribution-NonCommercial-No Derivative Works 4.0 International License](#).

Hysteresis and Anchoring Energy in Ferroelectric Liquid Crystals

YU. P. PANARIN

Organic Intermediates and Dyes Institute B. Sadovaya, 1/4, Moscow, 103787, Russia

The frequency dispersion of the coercive force of Ferroelectric Liquid Crystals (FLC) cells has been detected and examined in the range of infralow (lower than 0.1 Hz) frequencies. To clarify the low-frequency dispersion, the model has been suggested, based on the arrangement of free charges and well describing the experimental curves. The method for determination of the energy of FLC anchoring at the surface, developed on the basis of the static hysteresis loop, has been proposed. The dependence of bistability and the anchoring energy upon the orientant layer thickness has experimentally been investigated.

INTRODUCTION

Discovery of the electro-optical effect in Ferroelectric Liquid Crystals (FLC)¹ allowed or their application as a working medium in highly-multiplexed flat screens, including the television ones. The basic properties ensuring such an application of FLC are short switching time and bistability. In numerous investigations,²⁻⁵ it has been demonstrated that bistability is due to interaction of FLC with the surface. In connection with this, a necessity has arisen to develop a simple and reliable technique for measuring FLC anchoring energy. The earlier suggested methods for determining the anchoring energy are based upon: a shift of the phase transition temperature⁶, the static hysteresis loop⁵, the structural transitions between different states in FLC cells³ and the dynamics of the FLC director reorientation⁷. These works, however, either are purely theoretical or give only rough estimates.

We suggest a new approach to measuring the anchoring energy on the basis of the hysteresis loop.

DYNAMIC AND STATIC HYSTERESIS LOOPS

Our studies of the FLC cell hysteresis loops have shown that their form (shape) and width strongly depend on the frequency of the external voltage – that is, dispersion of the coercive force is observed. This dependence, in the range of high frequencies ($f > 0.1$ Hz), has been studied in detail in Ref. 8, and is related to the dynamics of

the FLC director switching. The width of the hysteresis loop W depends on frequency in the following way:⁸

$$W = \sqrt{U_o^2 - \left[U_o + \frac{\omega}{k} \log(\operatorname{tg}(\phi_0/2)) \right]^2} \quad (1)$$

where U_o is the amplitude of the external voltage applied to the cell, $k = P_s / \gamma_d$, ω is the angular frequency, P_s is the spontaneous polarization, γ is the rotational viscosity, ϕ_0 is the azimuthal pretilt angle. From the formula, it appears that at $\omega \rightarrow 0$ the loop width does not depend on frequency — that is, a static hysteresis loop is realized. In the experiment, however, dispersion is observed also in the range of infralow frequencies. In Figure 1 are presented the experimental dependencies of coercive force upon the frequency of external voltage of triangular form. As appears from the appended drawing, the static hysteresis is observed only in the single case (see Figure 1). In most cases, the dispersion curve exhibits one or two inflection points and does not show a saturation. We have applied the model of excess free charges^{9,10} to elucidating the dispersion of coercive force in the range of infra-low ($f < 0.1$ Hz) frequencies. The electric field inside the cell E is a sum of the field induced by the external voltage E_{out} and the field due to the free charges distributed between the electrodes of the cell E_{pol} ⁹

$$E(t) = \frac{U_{out} \varepsilon'}{2d\varepsilon + d\varepsilon'} + \frac{2\sigma_s(t)d'}{2d\varepsilon + d\varepsilon'} \quad (2)$$

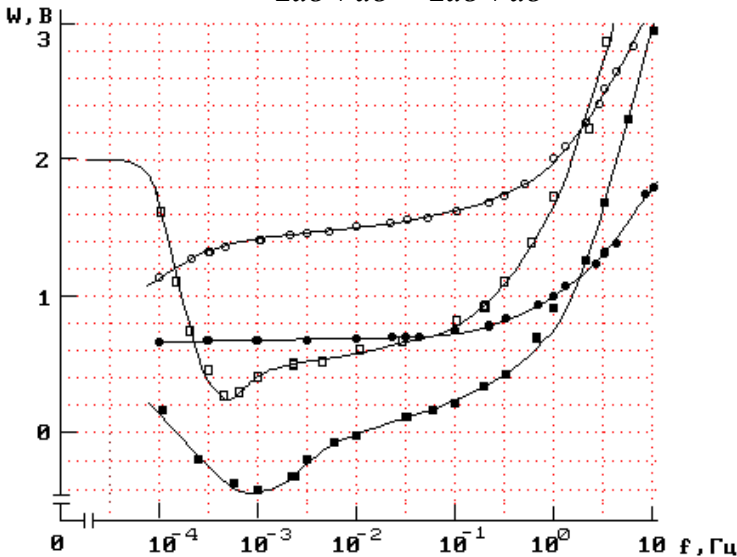


FIGURE 1. Frequency dependences of the hysteresis width W for different thicknesses of orientant layer d' : ■ - $d'=650\text{\AA}$, □ - $d'=300\text{\AA}$, ○ - $d'=200\text{\AA}$, ● - $d'=30\text{\AA}$

where ε , ε' and d , d' are the dielectric permittivity and the thickness of the FLC cell and the orientant layer respectively, U_{out} is the external voltage, σ_s is the surface density of charges on the cell electrodes.

For describing the free charge distribution process we have applied the simplest continuity equation⁹ with allowance made for the process of ionization and recombination:

$$\frac{\partial n(t)}{\partial t} = -n(t) \cdot E(t) \cdot \mu / d \quad (3)$$

where n , μ are the concentration and the mobility of free charges respectively.

Solving numerically coupled equations, we have obtained series of dependencies $E(t)$ upon different parameters: f , U_0 , μ , n . In Figure 2 are presented the curves of calculated voltage inside the cell $U(t)$ depended on the external voltage of different frequencies. As seen from the figure, at high frequencies the field induced by conductivity ions enhances the external field, whereas at low frequencies it diminishes that field. Thus the internal field might be either greater or smaller than the external one, which leads to a change in coercive force. In calculating the dispersion curves, the experimentally measured values of n_0 ($5 \cdot 10^{14} - 5 \cdot 10^{15} \text{ cm}^{-3}$) and μ ($10^{-9} - 10^{-8} \text{ cm}^2 \text{ S}^{-1} \text{ V}^{-1}$) were used. As appears from Figure 1, the calculated curves of dispersion of the coercive force are in good agreement with the experimental points. Moreover, the calculation predicts coercive force saturation for frequencies lower than 10^{-5} Hz and $n_0 < 10^{14} \text{ cm}^{-3}$ (see Figure 1).

Hence, taking into account the influence of conductivity ions, it is possible to correct the hysteresis loop at low frequencies and obtain the static hysteresis loop. From the experimental data, it is obvious (see Figure 1) that the hysteresis loops that are closest to the static ones are obtained at frequency 0.01 Hz.

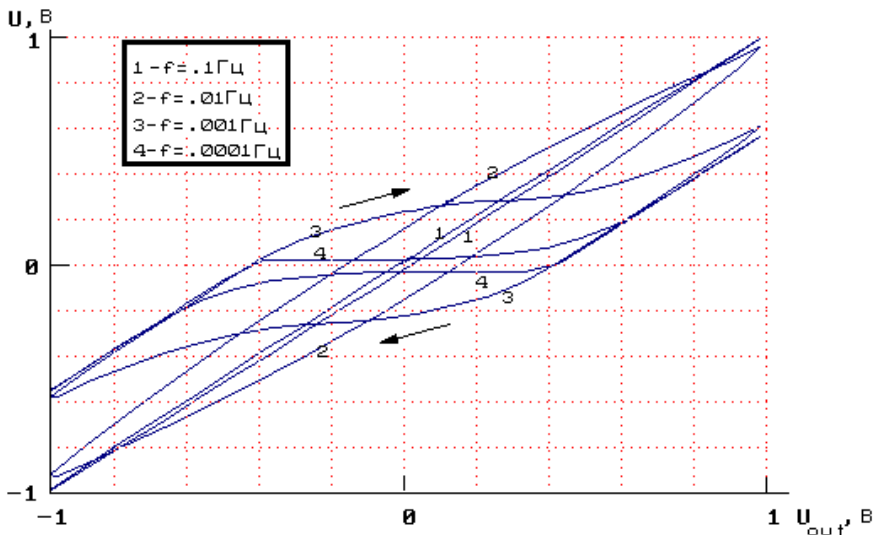


FIGURE 2. Calculated curves of internal voltage U hysteresis dependent upon the frequency of the external voltage U_{out}

ANCHORING ENERGY

Bistability in the electrooptical light modulators on FLC is provided by a corresponding interaction between the FLC molecules and the confining surfaces.

Clark and Lagerwall suggested the following form for the anchoring energy:

$$F_S = -\gamma_p \cdot \cos \phi - \gamma_d \cdot \cos^2 \phi \quad (4)$$

In addition, near the surface layer there arise elastic deformations due to FLC orientation contouring the relief of a rubbed orientant. The free energy corresponding to the surface deformation is described by formula:¹¹

$$F_{ds} = (K/4) \cdot u_s^2 q_s^2 \sin^2 \alpha \quad (5)$$

where u_s and q_s are the depth and the wave vector of the surface relief of the sinusoidal form respectively, K is the elastic constant of FLC in a one-constant approximation, α is the angle between the projection of N director on the electrode plane and the rubbing direction \mathbf{R} . If the FLC is oriented such that smectic layers are perpendicular to the electrodes plane, then angle α is related to angles θ and ϕ by the following relation:

$$\alpha = \arcsin(\sin \theta \cdot \cos \phi) \approx \theta \cdot \cos \phi \quad (6)$$

Taking into account the expressions (5) and (6), and the energy of interaction of the FLC with the rubbed surface, it is possible to write the following expression:

$$F_S = (K^* - \gamma_d) \cos^2 \phi - \gamma_p \cos \phi \quad (7)$$

where $K^* = (K/4) \cdot u_s^2 q_s^2 \theta$ is the surface elasticity of FLC.

The results of a study of the director switching process in the FLC cells under low ($E < 5 \text{ V}/\mu$) fields have demonstrated that after field reversal first there arise domains of the opposite sign ($\phi = 0$ or $\phi = \pi$) then domains grow in size and finally a completely uniform state is achieved. In this case, $\partial\phi/\partial x = 0$ in all the domains with exception of domain walls.

Taking into account the aforesaid and neglecting the elastic energy of domain walls the surface density of the free energy of a FLC cell (in the case of two similar surfaces) can be written in the following form.

$$F_S = 2\gamma_q \cos^2 \phi - P_s U \cdot \cos \phi \quad (8)$$

where $\gamma_q = (K^* - \gamma_d)$ is the quadratic anchoring energy. This function exhibits an extreme point (within the range $0 < \phi < \pi$):

$$\phi^* = \arccos(P_s U / 4\gamma_q) \quad (9)$$

If $\gamma_q < 0$, then ϕ^* correspond to the maximum of free energy and the cell possesses hysteresis properties, but if $\gamma_q > 0$, then ϕ^* correspond to the minimum and the cell possesses no hysteresis. A disadvantage of the aforesaid simple model consists in that it described only the rectangular form of the hysteresis loop with the switching at $U = \pm U_C = \pm 4 \gamma_q / P_s$, and, moreover, it does not explain the cause of different domain existence in intermediate states. To eliminate this inconsistency of the model with

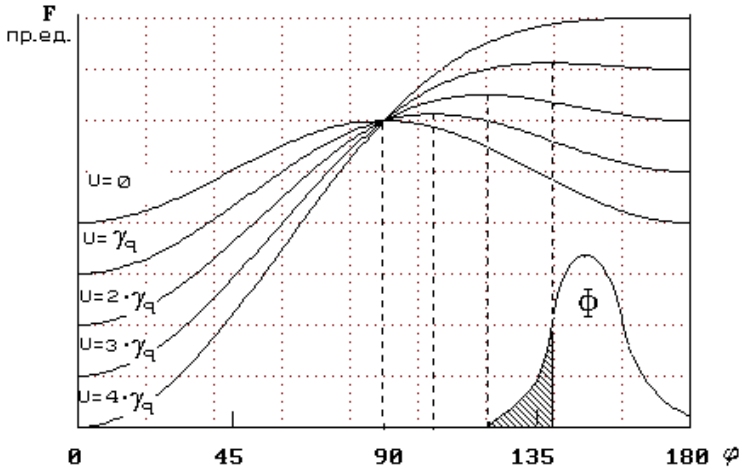


FIGURE 3 Dependence of the surface density of free energy $F(\phi)$ upon the voltage across a FLC cell, U_{out} . $\Phi(\phi_0)$ is function of distribution of the azimuthal tilt angle ϕ_0 .

the experiment we suggest that in a real cell in the homogeneous state, vector \mathbf{P}_s is not exactly perpendicular to the electrode plane, but exhibits some pretilt angle ϕ_0 . Furthermore, because of non-ideal orientation the pretilt angle is different at the different points of the cell — that is, there is some distribution $\Phi(\phi_0)$ according to the azimuthal pretilt angle. The normalizing condition is as follows:1

$$\int_0^\pi \Phi(\phi_0) d\phi_0 = 1 \quad (10)$$

In Figure 3 are presented the dependencies of the free energy at various voltages applied to the cell. From the appended drawing, it is obvious that at $U < 4 \gamma_q/P_s$ some regions are located to the left of the maximum of the function of free energy. Domains of the opposite sign arise in those regions. At voltage $U = 4 \gamma_q/P_s$ the maximum $\phi_0 = \pi$ and all the regions transform into state $\phi = 0$. Thus, on having measured the saturation voltage U_s , it becomes possible to determine the anchoring energy:

$$\gamma_q = P_s U_s / 4 \quad (11)$$

In practice, the voltages U_s and U_c differ from each other by about 10 to 30%.

On the basis of the aforesaid, hysteresis of macroscopic polarization P^* is described by the following formula:

$$P^* = 1 - 2 \cdot \int_0^{\phi^*} \Phi(\phi_0) d\phi_0 \quad (12)$$

In accordance with the model, the shape of domains depends upon the character of disturbance of the azimuthal pretilt angle. Three different causes of such a

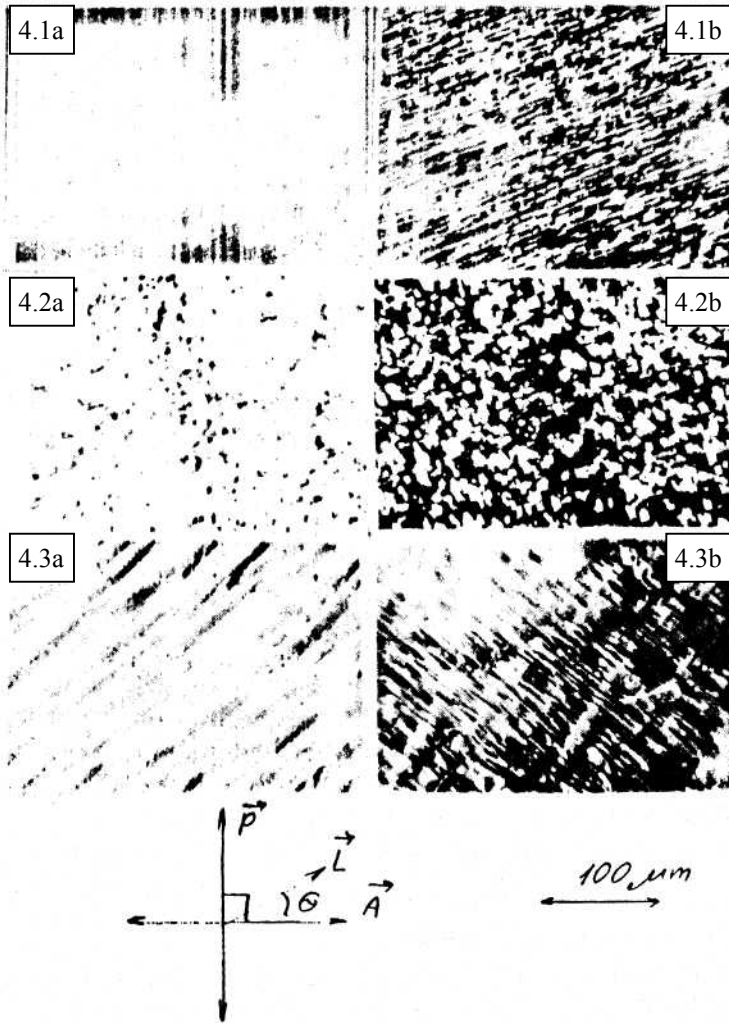


FIGURE 4. Microphotographs of FLC cells in crossed polarizers. Cell parameters: (4.1) $d = 5 \mu$, $d' = 300 \text{ \AA}$; (4.2) $d = 1.2 \mu$, $d' = 30 \text{ \AA}$; (4.3) $d = 15.5 \mu$, $d' = 200 \text{ \AA}$. P - polarizer axis, A - analyzer axis, L—smectic layer normal, θ —smectic tilt angle.

disturbance are possible (Figure 4):

- (1) *Stripe-shaped domains*¹²⁻¹⁷ (see Figure 4.1). In relatively thin cells ($d < 15 \mu$), the characteristic lines of orientation disturbance are directed along the rubbing direction (see Figure 4.1 a). The domains arising during the switching process possess a similar shape (see Figure 4.1 b).
- (2) *Surface domains* (Figure 4.2). Pointlike orientation defects are predominant in thin ($d < 3 \mu$) cells with a thin ($d' < 100 \text{ \AA}$) orientant layer (see Figure 4.2a). In this case, the domains do not possess any preferable direction (see Figure 4.2b).

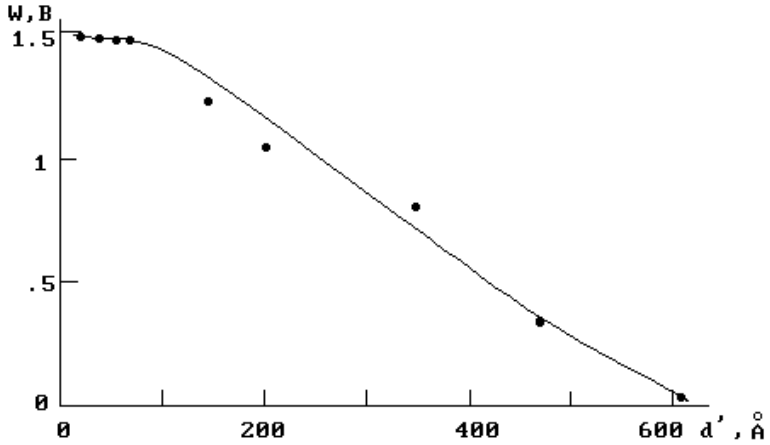


FIGURE 5 Dependence of the hysteresis loop width W and the anchoring energy γ_q on the thickness of the PVA orientant layer d' .

- (3) *Ferroelectric domains* (Figure 4.3). Recently,^{18,19} it has been shown that a modulation of angle ϕ_0 in direction perpendicular to the smectic layers exist in sufficiently thick ($d > 10\mu$) cells. This does show up by the presence on the bright background of dark lines parallel to the smectic layers (see Figure 4.3a). The growth of domains of the reversed sign originates from those lines (see Figure 4.3b).

Thus, the bistable properties and hysteresis of the FLC cells are determined by the quadratic anchoring energy γ_q rather than merely by its dispersion part. However, there exist a possibility of measuring the proper dispersion anchoring energy γ_d . As follows from formulas (5)-(8), the energy of surface deformations K^* decreases with d' and at $d' = 0$ the quadratic part of anchoring energy is equal to the dispersion one, thus:

$$\lim_{d' \rightarrow 0} \gamma_q = \gamma_d \quad (13)$$

In Figure 5 is presented experimental dependence of the anchoring energy γ_q upon the thickness of the PVA orienting coating layer. The value of γ_q decreases in its modulus as the orientant thickness increases, and finally reversed its sign, instability disappearing in this case. The experimental data are in good agreement with the aforesaid concepts.

REFERENCES

1. N.A. Clark, S.T. Lagerwall. *Appl. Phys. Lett.*, **36**, 899 (1980).
2. M.A. Handsy, N.A. Clark, S.T. Lagerwall, *Phys. Rev. Lett.*, **51**, 471 (1983).
3. M. Isogai, K. Kondo, Sh. Nonaka, M. Odamura and A. Mukoh, *Proc. of 1985 Intern. Disp. Conf.*, 225 (1985).
4. G. Derfel, *Liq. Cryst.*, **8**, 331 (1990).
5. J. Dijon, C. Ebel, L. Mulatier and D. Leti-Irudi. *Ferroelectrics*, **85**, 47 (1988).
6. D.F. Aliev and A.R. Imamaliyev, *Liq. Cryst.*, **4**, 423 (1989).
7. P. Schiller, *Cryst. Res. Technol.*, **21**, 301 (1986).
8. C. Reynaerts and A. de Vos, *Ferroelectrics*, **113**, 439 (1991).
9. K.H. Yang, T.C. Chien and S. Osofsky, *Appl.Phys.Lett.*, **55**, (1989).
10. K.H. Yang and T.C. Chien, *Jpn.J.Appl.Phys.*, **28**, L-1599 (1989).
11. D. Berreman, *Phys. Rev. Lett.*, **28**, 1683 (1972).
12. J. Pavel and M. Glogarova, *Ferroelectrics*, **113**, 619 (1991); *Liquid Crystals*, **9**, 87 (1991).
13. M. Kleman, *Points, Lines, Walls in Liquid Crystals; Magnet is System and Various Ordered Media*, Wiley, N.Y., 1983.
14. L. Lejcek and S. Pirkl, *Liquid Crystals*, **8**, 871 (1990).
15. A. Jakli and A. Saupe, Lecture at *Third Int. Conf. on Ferroelectric Liquid Crystals*, Boulder, 1991.
16. A. Verhulst and F. Stommels, *Ferroelectrics*, **121**, 79 (1991).
17. R.F. Shao, P.C. Willis and N.A. Clark, *Ferroelectrics*, **121**, 127 (1991).
18. L.A. Beresnev, M.V. Loseva, N.I. Chrnova, S.G. Kononov, P.V. Adomenas and E.P. Pozhidaev, *Pisma Zh. Tekh. Fiz.*, **51**, 457 (1990).
19. L.A. Beresnev, M. Pfeifler, W. Haase, M.V. Loseva, R.I. Chernova and P.V. Abdomenas, *Pis'maZh. Tekh. Fiz.*, **53**, 170(1991).